

Dear Editor,

We hereby submit the amended version of the manuscript. We have done some significant changes in the intro, results and discussion section. These changes include addition of a sub-section (5.3) to discuss the potential significance of ridge push stresses on fluid dynamics in the context of additional factors likely contributing to the total state of stress in the region. As explained before, the study does not aim at quantifying the different factors causing regional stresses but at evaluating the significance of tectonic stresses on seepage activity. We have thus amended the text in the abstract, the intro, the results and discussion and the conclusion sections to clarify that we argue for a significant effect of tectonic stresses on fluid dynamic without neglecting the significance of other potential sources of stress in the region. We hope this address the major concern by referee one (i.e., that it cannot be concluded that tectonic stresses have a dominant effect on fluid migration in the region before quantifying all potential sources of stress). In addition, we included a short outlook section (7) to indicate important to work that remains to be done and that is planned to further assess the effect of stresses on fluid dynamics in the region.

Please see below a point by point response to the referee comments and the marked-up version of the manuscript.

Sincerely,

Andreia Plaza-Faverola and Marie Keiding

*As pointed out in my review of the original version of this paper, authors rightfully point out that the local stress field, where seepage occurs, may results from four different loading processes:*

*A: gravitational effects through topography effects and density contrasts;*

*B: Flexural effects due to sediment erosion and deposition;*

*C: Glacially flexural effects;*

*D: tectonic stresses resulting from the Vestnesa Ridge.*

*Authors claim that by investigating solely the ridge push effect they can demonstrate that it is the most significant effect that controls methane production. In order to undertake this demonstration they propose to use Okada 's elastic solution that addresses stresses caused by a dislocation in an homogeneous infinite plate.*

**Reply: we do not claim that mid-ocean ridge stress has the most significant effect on seepage; we hypothesize that mid-ocean ridge stress has a significant effect (possibly a dominant effect) on seepage (specifically on the Vestnesa sedimentary ridge; we are not hypothesizing that it is necessarily the case for the entire west Svalbard margin). Additional sources of stress are listed in the paper and it is clearly pointed out that we do not aim at quantifying all the sources of stress in the region.**

**Action: We rephrased the text in places to make even more emphatic that we are postulating tectonic stress as a significant factor affecting seepage activity, without disregarding that other sources of stress can as well have a significant effect on fluid migration in the region. We have added a new sub-section (5.3) in the results and discussion section to discuss explicitly other potential sources of stress in comparison to the tectonic stresses.**

*I pointed out in my review that, in elastic theory, when various loading processes are applied on the same volume of an elastic material, the resulting stress fields is the sum of that caused by each of the various loading processes applied separately. In the present case, authors must demonstrate that effects of A+B+C are negligible as compared to that of D, their push ridge model, if they wish to conclude that only D is of import. But they fail to do so.*

**Reply: we do not conclude that only the mid-ocean ridge spreading related stresses are of importance.**

**Action: please see previous comment.**

*Interestingly, authors mention in their introduction that Wallman et al. (2018) conclude that hydrate dissociation off Svalbard is induced by isostatic glacial rebound. So clearly not everybody agrees with their proposition that glacial rebound is negligible.*

**Reply: the study by Wallmann et al., is used for presenting the latest hypothesis for explaining seepage in a region restricted to the shelf break: that gas hydrates dissociate due to post glacial isostatic rebound. This hypothesis first, is relevant only to this region close to the shelf break where the gas hydrate stability zone pinches out and small changes in pressure and temperature easily bring hydrates out of stability (see for example the analyses of pressure changes affecting the gas hydrate reservoir along the Vestnesa Ridge by Plaza-Faverola et al., 2017). It is not valid for > 1000 m water depth, towards the Vestnesa Ridge, where the gas hydrates are perennially stable. Second, the hypothesis does not discuss horizontal stresses, it claims decrease in the hydrostatic pressure is the cause of hydrate dissociation. Third, gas hydrates has not been found in this seepage region.**

**Action: we have rephrased the text where we used the reference Wallmann et al., 2018 to emphasize that glacial stresses are actually an additional explanation for sustaining present day seepage at the shelf-break region; something that Wallmann et al. actually disregard.**

*Before addressing the stress analysis proposed by authors for the ridge push effect, I will point out that topography effects at a depth of 1200 m is of particularly import given the bathymetry shown on figure 1 , which indicates a slope extending from -1 km to -3km below sea level. Clearly the stress field close to this free surface depends strongly on topography and its effect must be analyzed properly before claiming it is negligible.*

**Reply: we agree that a gravitational component in the faults at the flanks of the Vestnesa basin and on the crest of Vestnesa Ridge is probable. We do indicate this. Nevertheless, the tectonic origin of the faults is put forward based on previous studies observations and our detailed seismic imaging of the faults suggesting that the Knipovich ridge rift system is propagating northward (see Crane et al., 2001; Vanneste et al., 2005; Hustoft et al., 2009; Plaza-Faverola et al., 2015).**

**Action: this is now more explicitly discussed in the new discussion section. Please see action for the first comment.**

*In Appendix A, Okada's dislocation is embedded in the ductile part of the crust. This is precisely contradictory with the elastic hypothesis of Okada's solution and renders the stress analysis erroneous. In addition, it is stated, p 4 - second paragraph, that the total sedimentary thickness is larger 5 km. Elastic characteristics of sediments differ strongly from that of basement crystalline rocks so that the homogeneous semi-infinite space analysis does not apply for the elastic part of the crust.*

**Reply:** The Okada solution has previously been used to correctly model the stresses in the elastic crust by simulating the continuous deformation below the brittle-ductile transformation zone (Arnadottir et al, 2009). We again point out that the modelled stresses agree very well with stress indications from earthquake focal mechanisms in the region. The reviewer points out that the elastic parameters of sediments vary from the elastic parameters of the crystalline rocks, which we acknowledge. Differences in elastic parameters will result in different magnitudes of stress, but not affect the directions and relative stress magnitudes presented in this study.

Action: we added text and rephrased in places to better describe the simplifying assumptions and also point out that this study is a first attempt to assess the influence of tectonic stress,

*In conclusion, first the stress field analysis of the ridge push effect is erroneous, second the proposition that topography effects are negligible has not been demonstrated, third results from Wallman et al. show that glacial rebound is an important factor controlling methane production off Svalbard.*

**Reply:** See comments above.

My final recommendation is not to publish this paper.

1 **CORRELATION BETWEEN TECTONIC STRESS REGIMES AND METHANE SEEPAGE ON THE**  
2 **WEST-SVALBARD MARGIN**

3  
4 A. Plaza-Faverola<sup>1</sup> and M. Keiding<sup>2</sup>

5 <sup>1</sup> CAGE-Centre for Arctic Gas Hydrate, Environment, and Climate; Department of Geosciences, UiT The Arctic  
6 University of Norway, N-9037 Tromsø, Norway

7 <sup>2</sup> Geological Survey of Norway (NGU), P.O. Box 6315 Torgarden, 7491 Trondheim, Norway

8 *Correspondence to:* Andreia Plaza-Faverola (Andreia.a.faverola@uit.no)

9 **Abstract.** Methane seepage occurs across the west-Svalbard margin at water depths ranging from the upper shelf  
10 at < 300 m to gas hydrate systems in the deep sea at > 1000 m. The Vestnesa sedimentary ridge, located on oceanic  
11 crust at 1000-1700 m water depth, hosts a perennial gas hydrate and associated free gas system. Present day seepage  
12 activity is restricted to the eastern segment of the sedimentary ridge, despite morphological and paleontological  
13 evidence for past seepage activity along the entire ridge extent. An eastward transition from the zone with clear  
14 morphological evidence of past seepage to the zone of active present-day seepage coincides with a change in the  
15 faulting pattern of near-surface strata. We modelled the tectonic stress regime exclusively due to oblique spreading  
16 along the Molloy and Knipovich spreading ridges to investigate whether spatial and temporal variations in the  
17 spreading-related stress field may explain patterns of seepage distribution.

18 The model reveals a zone of tensile stress that extends northward from the Knipovich Ridge and encompasses a  
19 zone of active gas chimneys and pockmarks on the eastern Vestnesa Ridge. The seemingly inactive part of the  
20 Vestnesa Ridge is presently located in a strike-slip regime. Modelled stresses due to oblique spreading suggest that  
21 minimum principal stresses are perpendicular to mapped NW-SE oriented faults along the Vestnesa Ridge, thus  
22 favouring opening of pre-existing faults and fractures. Seepage may occur by leakage from the base of the gas  
23 hydrate stability zone if pore fluid pressure dominates over horizontal stresses. It is likely that glacial stresses have  
24 significantly contributed to the total state of stress during glaciations, possibly explaining multiple seepage events  
25 along the entire extent of the gas-charged Vestnesa Ridge. The contribution of other factors such as flexural bending  
26 to the total state of stress remains to be investigated. Our study provides a first order assessment of how tectonic  
27 stresses may be influencing the kinematics of near-surface faults and associated seepage activity offshore the west-  
28 Svalbard margin.

29  
30

~~The model reveals a zone of tensile stress that extends northward from the Knipovich Ridge and encompasses the zone of extensional faulting and associated active seepage on the eastern Vestnesa Ridge segment. The seemingly inactive part of the ridge is presently located in a strike slip regime. Our modelling results suggest that it can be explained by opening of faults and fractures favourably oriented with respect to spreading related principal stresses, where pore fluid pressure overcomes the horizontal stress. Multiple seepage events along the entire extent of the gas charged Vestnesa Ridge, may have been incited by favourably oriented mid-ocean ridge derived stresses in the past or by additional sources of stress related for example to glacial isostasy. Our study provides a first order assessment of how stresses from mid-ocean ridge spreading may be influencing the kinematics of near surface faults and associated seepage activity offshore the west Svalbard margin.~~

## 1. INTRODUCTION

Seafloor seepage is a wide-spread phenomenon which consists in the release of natural gases into the oceans. Hundreds of gigatonnes of carbon are stored as gas hydrates and shallow gas reservoirs in continental margins (e.g., Hunter et al., 2013). The release of these carbons over geological time is an important component of the global carbon cycle. Understanding and quantifying seepage has important implications for ocean acidification, deep-sea ecology and global climate. Periods of massive methane release from gas hydrate systems (e.g., Dickens, 2011) or from large volcanic basins like that in the mid-Norwegian Margin (e.g., Svensen et al., 2004) have been linked to global warming events such as the Palaeocene-Eocene thermal maximum. We know that methane seepage has been occurring for millions of years, but we have a poor understanding of what forces it.

Present day seepage is identified as acoustic flares in the water column commonly originating at seafloor depressions, while authigenic carbonate mounds are used as indicators of longer-term seepage activity (e.g., Judd and Hovland, 2009). Seepage at the theoretical upstream termination of the gas hydrate stability zone (GHSZ) (i.e., coinciding with the shelf edge) on different continental margins, has been explained by temperature driven gas-hydrate dissociation (e.g., Skarke et al., 2014; Westbrook et al., 2009). On formerly glaciated regions of Svalbard and the Barents Sea margins, active seepage ~~has been explained by gas hydrate dissociation either due is believed to be associated with~~ to pressure changes resulting from the retreat of the ice-sheet (e.g., Andreassen et al., 2017; Portnov et al., 2016) ~~or to. The effect of post-glacial~~ ion uplift ~~on gas hydrate stability has been recently suggested~~

60 ~~as an alternative explanation for seepage localized at the shelf break offshore west Svalbard~~ (Wallmann et al.,  
61 2018)

62  
63 Across the formerly glaciated west-Svalbard margin, active seepage extends beyond the shelf break and the region  
64 formerly covered by ice. As a matter of fact, active seepage sites have been identified from inside Isfjorden (Roy  
65 et al., 2014) to water depths of ~1200 m (Smith et al., 2014) where the Vestnesa Ridge hosts a perennially stable  
66 gas hydrate system ~~beyond > 50 km seaward from~~ the ice-sheet grounding line. The Vestnesa Ridge is a NW-SE  
67 oriented contourite deposit located between the northward termination of the Knipovich ridge and the eastern flank  
68 of the Molloy spreading ridge in the Fram Strait (Fig. 1). Seafloor pockmarks along the Vestnesa Ridge, first  
69 documented by Vogt (1994), exist along the entire ridge. However, acoustic flares have been observed to originate  
70 exclusively at large pockmarks located on the eastern part of the sedimentary ridge (Fig. 2, 3). The presence of  
71 inactive pockmarks adjacent to a zone of active seepage along the Vestnesa Ridge, raises the question what stopped  
72 previously active seepage sites?

73  
74 Plaza-Faverola et al., (2015) documented seismic differences in the orientation and type of faulting along the ridge  
75 and showed a link between the distribution of gas chimneys and faults. They postulated that the faults have a  
76 tectonic origin and that spatial and temporal tectonic stress variations may have a long-term effect on the spatial  
77 distribution of fault-related gas migration and seepage evolution. In general, the total state of stress at passive  
78 continental margins is the result of diverse factors including bathymetry and subsurface density contrasts,  
79 subsidence due to sedimentary loading and lithospheric cooling, in addition to ridge-push (e.g., Turcotte et al.,  
80 1977). The state of stress at formerly glaciated margins (i.e., such as the west-Svalbard margin) has in addition the  
81 effect of flexural bending succeeding ice-sheet advances and retreats (e.g., Fjeldskaar and Amantov, 2018;  
82 Grunnaleite et al., 2009; Patton et al., 2016). The interaction between the above mentioned factors renders  
83 modelling of the total state of stress a complex problem that has not been tackled. In this study, we focus exclusively  
84 on the potential contribution of oblique spreading at the Molloy and the Knipovich ridges to the total stress state  
85 along the Vestnesa Ridge and do a qualitative analysis of how these stresses may be influencing seepage activity.

86  
87 The effect of regional stresses on fluid dynamics in the near-surface has implications for seepage systems globally.  
88 Splay-faults are found to sustain shallow gas accumulations and seepage (Plaza-Faverola et al., 2016), and the  
89 relationship between fault kinematics and fluid migration has been documented specially at accretionary margins  
90 where earthquake-induced seafloor seepage has been observed (e.g., Geersen et al., 2016). So far the information

91 about the present day stress regime in the Fram Strait has been limited to large scale lithospheric density models  
92 (Schiffer et al., 2018) and a limited number of poorly constrained stress vectors from earthquake focal mechanisms  
93 (Heidbach et al., 2016). Our study provides a first order assessment of how stresses from slow spreading mid-ocean  
94 ridges may be influencing the kinematics of near-surface faults and associated seepage activity in a passive Arctic  
95 margin.

96 Plaza Faverola et al., (2015) documented seismic differences in the orientation and type of faulting along the ridge  
97 and showed a link between the distribution of gas chimneys and faults. They postulated that spatial and temporal  
98 tectonic stress variations have a long term effect on the spatial distribution of fault related gas migration and  
99 seepage evolution. ~~The information about the present day stress regime in the Fram Strait is limited to large scale~~  
100 ~~lithospheric density models (Schiffer et al., 2018) and a limited number of poorly constrained stress vectors from~~  
101 ~~earthquake focal mechanisms (Heidbach et al., 2016). Here, we experiment with an approach that allows us to~~  
102 ~~approximate the orientation and type of stress regimes exclusively due to oblique spreading at Molloy and~~  
103 ~~Knipovich Ridges. We study, qualitatively, how stresses from mid-ocean ridge spreading alone may be influencing~~  
104 ~~the kinematics of near-surface faults and associated methane seepage activity;~~

105  
106 ~~The effect of regional stresses on fluid dynamics in the near surface has implications for seepage systems globally.~~  
107 ~~The relationship between fault kinematics and fluid migration has been documented specially at accretionary~~  
108 ~~margins where earthquake induced seafloor seepage has been monitored (e.g., Geersen et al., 2016) and splay-~~  
109 ~~faults are found to sustain shallow gas accumulations and seepage (Plaza Faverola et al., 2016). The information~~  
110 ~~about the present day stress regime in the Fram Strait is limited to large scale lithospheric density models (Schiffer~~  
111 ~~et al., 2018) and a limited number of poorly constrained stress vectors from earthquake focal mechanisms~~  
112 ~~(Heidbach et al., 2016). With the present study we show, using an Arctic case, that seepage on passive continental~~  
113 ~~margins may be affected as well by the stress regime resulting from mid-ocean ridge spreading.~~

114

## 115 2. STRUCTURAL AND STRATIGRAPHIC SETTING OF THE VESTNESA RIDGE

116 In Fram Strait, sedimentary basins are within tens of kilometres from ultra-slow spreading Arctic mid-ocean ridges  
117 (Fig. 1). The opening of the Fram Strait was initiated 33 Ma ago and evolved as a result of slow spreading of the  
118 Molloy and Knipovich Ridges (Engen et al., 2008). An important transpressional event deformed the sedimentary  
119 sequences of western Svalbard, resulting in folds and thrustbelts, during the Paleocene-Eocene dextral movement  
120 of Spitsbergen with respect to Greenland. Transpression stopped in the early Oligocene when the tectonic regime

121 became dominated by extension (Myhre and Eldholm, 1988). The circulation of deep water masses through Fram  
122 Strait started during the Miocene, ca. 17-10 Ma ago (Ehlers and Jokat, 2009; Jakobsson et al., 2007), establishing  
123 the environmental conditions for the evolution of bottom current-driven sedimentary drifts (Eiken and Hinz, 1993;  
124 Johnson et al., 2015). It has been suggested that the opening of the northern Norwegian–Greenland Sea was initiated  
125 by the northward propagation of the Knipovich ridge into the ancient Spitsbergen Shear Zone (SSZ) (Crane et al.,  
126 1991).

127

128 The continental crust beneath the western coast of Svalbard thins towards the Hornsund Fault zone (HFZ) indicating  
129 extension following the opening of the Greenland Sea (Faleide et al., 1991). Late Miocene and Pliocene  
130 sedimentation, driven by bottom currents, resulted in the formation of the ca. 100 km long Vestnesa Ridge between  
131 the HFZ off west-Svalbard and oceanic crust highs at the eastern flank of the Molloy mid-ocean ridge (Eiken and  
132 Hinz, 1993; Vogt et al., 1994). The sedimentary ridge is oriented parallel to the Molloy Transform Fault (MTF)  
133 and its crest experiences a change in morphology from narrow on the eastern segment to expanded on the western  
134 Vestnesa Ridge segment (Fig. 2). The exact location of the continental-ocean boundary remain somewhat uncertain  
135 (Eldholm et al., 1987) but it is inferred to be nearby the transition from the eastern to the western segments (Engen  
136 et al., 2008).

137

138 The total sedimentary thickness along the Vestnesa Ridge remains unconstrained. Based on one available regional  
139 profile it can be inferred that the ridge is > 5 km thick in places (Eiken and Hinz, 1993). It has been divided into  
140 three main stratigraphic units (Eiken and Hinz, 1993; Hustoft, 2009): the deepest sequence, YP1, consists of synrift  
141 and post-rift sediments deposited directly on oceanic crust; YP2 consists of contourites; and YP3, corresponding  
142 to the onset of Pleistocene glaciations (ca. 2.7 Ma ago) (Mattingsdal et al., 2014), is a mix of glaciomarine  
143 contourites and turbidites. The effect of ice-sheet dynamics on the west-Svalbard margin (Knies et al., 2009; Patton  
144 et al., 2016) has influenced the stratigraphy, and most likely the morphology, of the Vestnesa Ridge and adjacent  
145 sedimentary basins. In this Arctic region, glaciations are believed to have started even earlier than 5 Ma ago. The  
146 onset of local intensification of glaciations is inferred to have started ca. 2.7 Ma ago (e.g., Faleide et al., 1996;  
147 Mattingsdal et al., 2014). Strong climatic fluctuations characterized by intercalating colder, intense glaciations with  
148 warmer and longer interglacials, dominated the last ca. 1 Ma. (e.g., Jansen and Sjøholm, 1991; Jansen et al., 1990).

149

150 A set of N-S to NNE-SSE trending faults cut the recent strata at a narrow zone between the Vestnesa Ridge and  
151 the northern termination of the KR (Fig 1). Due to their structural connection with the KR they are believed to

152 indicate ongoing northward propagation of the rift system. High resolution 3D seismic data collected on the eastern  
153 Vestnesa Ridge segments revealed sub-seafloor NW-SE oriented faults (i.e., near-vertical and parallel to the  
154 sedimentary ridge axis) that could be genetically associated with the outcropping faults (Plaza-Faverola et al., 2015;  
155 Fig. 2). Comparison of similar high resolution 3D seismic data from the western Vestnesa Ridge segment shows  
156 that the style of faulting has been radically different from that of the eastern segment. Here, only randomly oriented  
157 small fault segments are revealed in nevertheless pockmarked Holocene strata (Fig. 2). Gravimetric data also  
158 indicate an abrupt structural change to the west compared to the east of a N-S oriented fault separating the ridge  
159 segments (Plaza-Faverola et al., 2015).

160

161 The gas hydrate system dynamics along the Vestnesa Ridge seems to be highly influenced by spatial variations in  
162 the geothermal gradient and the gas composition (Plaza-Faverola et al., 2017). Thermogenic gas accumulations at  
163 the base of the GHSZ (Fig. 2) are structurally controlled (i.e., the gas migrates towards the crest of the sedimentary  
164 drift) and part of this gas sustains present day seepage activity (Bünz et al., 2012; Knies et al., 2018; Plaza-Faverola  
165 et al., 2017). Reservoir modelling shows that source rock deposited north of the MTF has potentially started to  
166 generate thermogenic gas 6 Ma ago and that migrating fluids reached the Vestnesa Ridge crest at the active seepage  
167 site ca. 2 Ma ago (Knies et al., 2018). It is suspected that seepage has been occurring, episodically, at least since  
168 the onset of the Pleistocene glaciations c. 2.7 Ma ago leaving buried pockmarks and authigenic carbonate crusts as  
169 footprint (Plaza-Faverola et al., 2015). Many transient seepage events are suspected and one was dated to ca. 17.000  
170 years based on the presence of a ~1000 years old methane-dependent bivalve community possibly sustained by a  
171 gas pulse through a fault (Ambrose et al., 2015).

### 172 3. SEISMIC DATA

173 The description of faults and fluid flow related features along the Vestnesa Ridge is documented in Plaza-Faverola  
174 et al., 2015. The description is based on two-3D high resolution seismic data sets acquired on the western and the  
175 eastern Vestnesa Ridge segments respectively, and one 2D seismic line acquired along the entire Vestnesa Ridge  
176 extent (Fig. 2 this paper). These data have been previously used for the investigation of BSR dynamics (Plaza-  
177 Faverola et al., 2017) and documentation of gas chimneys and faults in the region (Petersen et al., 2010; Plaza-  
178 Faverola et al., 2015). The data were acquired on board R/V Helmer Hanssen using the 3D P-Cable system (Planke  
179 et al., 2009). Final lateral resolution of the 3D data sets is given by a bin size of 6.25x6.25 m<sup>2</sup> and the vertical  
180 resolution is > 3 m with a dominant frequency of 130 Hz. Details about acquisition and processing can be found in  
181 Petersen et al., 2010 and Plaza-Faverola et al., 2015. For the 2D survey the dominant frequency was ~80 Hz

182 resulting in a vertical resolution  $> 4.5$  m (assumed as  $\lambda/4$  with an acoustic velocity in water of 1469 m/s given by  
183 CTD data; Plaza-Faverola et al., 2017).

#### 184 4. THE MODELING APPROACH

185

186 This study deals exclusively with tectonic stress due to ridge push. We use the approach by Keiding et al. (2009)  
187 based on the analytical solutions derived by Okada (1985), to model the plate motion and tectonic stress field due  
188 to spreading along the Molloy and Knipovich Ridges. ~~Because the model only incorporates plate spreading, the  
189 stresses resulting from the models cannot be considered as a representation of the total stress field in the region.  
190 However, the objective of this study is not to model the total stress field, rather, the focus is to investigate how  
191 tectonic stress may influence seepage in the proximity of the two spreading ridges. By excluding all other sources  
192 of stress in the modelling, we are able to investigate the influence of plate spreading exclusively.~~

193

194 The Okada model and our derivation of the stress field from it is described in more detail in appendix A. The  
195 Molloy and Knipovich Ridges are modelled as rectangular planes with opening and transform motion in a flat Earth  
196 model with elastic, homogeneous, isotropic rheology. Each rectangular plane is defined by ten model parameters  
197 used to approximate the location, geometry and deformation of the spreading ridges (Okada, 1985; see supplement  
198 Table 1). The locations of the two spreading ridges were constrained from bathymetry maps (Fig. 1). The two  
199 spreading ridges are assumed to have continuous, symmetric deformation below the brittle-ductile transition, with  
200 a half spreading rate of 7 mm/yr and a spreading direction of N125°E, according to recent plate motion models  
201 (DeMets et al., 2010). Because the spreading direction is not perpendicular to the trends of the spreading ridges,  
202 this results in both opening and right-lateral motion; that is, oblique spreading on the Molloy and Knipovich Ridges.  
203 The Molloy Transform Fault, which connects the two spreading ridges, trends N133°E, thus a spreading direction  
204 of N125°E implies extension across the transform zone. We use a depth of 10 km for the brittle-ductile transition  
205 and 900 km for the lower boundary of the deforming planes, to avoid boundary effects. For the elastic rheology,  
206 we assume typical crustal values of Poisson's ratio = 0.25 and shear modulus = 30 GPa (Turcotte and Schubert,  
207 2002). We perform sensitivity tests for realistic variations in 1) mid-oceanic spreading, 2) depth of the brittle-  
208 ductile transition, and 3) Poisson's ratio (Supplementary material). Variations in shear modulus, e.g. reflecting  
209 differences in elastic parameters of crust and sediments, would not influence the results, because we only consider  
210 the orientations and relative magnitudes of stress.

211

212 Asymmetric spreading has been postulated for the Knipovich Ridge based on heat flow data (Crane et al., 1991),  
213 and for other ultraslow spreading ridges based on magnetic data (e.g., Gaina et al., 2015). However, the evidence  
214 for asymmetry along the KR remains inconclusive and debatable in terms, for example, of the relative speeds  
215 suggested for the North American (faster) and the Eurasian (slower) plates (Crane et al., 1991; Morgan, 1981; Vogt  
216 et al., 1994). This reflects that the currently available magnetic data from the west-Svalbard margin is not of a  
217 quality that allows an assessment of possible asymmetry of the spreading in the Fram Strait (Nasuti and Olesen,  
218 2014). Thus, symmetry is conveniently assumed for the purpose of the present study.

219  
220 We focus on the stress field in the upper part of the crust (where the GHSZ is) and characterise the stress regime  
221 based on the relative magnitudes of the horizontal and vertical stresses. We refer to the stresses as  $\sigma_v$  (vertical  
222 stress),  $\sigma_H$  (maximum horizontal stress) and  $\sigma_h$  (minimum horizontal stress), where compressive stress is positive  
223 (Zoback and Zoback, 2002). A tensile stress regime ( $\sigma_v > \sigma_H > \sigma_h$ ) favours the opening of steep faults that can  
224 provide pathways for fluids. Favourable orientation of stresses with respect to existing faults and/or pore fluid  
225 pressures increasing beyond hydrostatic pressures are additional conditions for leading to opening for fluids under  
226 strike-slip ( $\sigma_H > \sigma_v > \sigma_h$ ) and compressive ( $\sigma_H > \sigma_h > \sigma_v$ ) regimes (e.g., Grault and Baleix, 1994).

227

#### 228 4. **RESULTS AND DISCUSSION**

##### 229 **54.1 PREDICTED STRESS FIELDS DUE TO OBLIQUE SPREADING AT THE MOLLOY AND** 230 **THE KNIPOVICH RIDGES**

231

232 The model predicts zones of tensile stress near the spreading ridges, and strike-slip at larger distance from the  
233 ridges. An unexpected pattern arises near the Vestnesa Ridge due to the interference of the stress from the two  
234 spreading ridges. A zone of tensile stress extends northward from the Knipovich Ridge, encompassing the eastern  
235 part of the Vestnesa Ridge. The western Vestnesa Ridge, on the other hand, lies entirely in a zone of strike-slip  
236 stress (Fig. 4).

237 The sensitivity tests show that the tensile stress zone covering the eastern Vestnesa Ridge is a robust feature of the  
238 model, that is, variations in the parameters result in a change of the extent and shape of the tensile zone but the  
239 zone remains in place (Supplementary material).

240

241

Formatted: Normal, Indent: Left: 0,63 cm, No bullets or numbering

Formatted: Font: (Default) +Headings (Times New Roman), 11 pt, Bold, All caps

Formatted: Font: (Default) +Headings (Times New Roman), 11 pt

242 ~~Sensitivity tests for realistic variations in 1) mid-oceanic spreading, 2) depth of the brittle-ductile transition, and 3)~~  
243 ~~elastic moduli, show that the tensile stress zone covering the eastern Vestnesa Ridge is a robust feature of the~~  
244 ~~model, that is, variations in the parameters result in a change of the extent and shape of the tensile zone but the~~  
245 ~~zone remains in place (Supplementary material).~~

246  
247 To investigate the geometric relationship between the predicted stress field and mapped faults, we calculated the  
248 orientations of maximum compressive horizontal stress (Lund and Townend, 2007). The maximum horizontal  
249 stresses ( $\sigma_H$ ) within the tensile regime approximately follow the orientation of the spreading axes (i.e., dominantly  
250 NE-SW to N-S; Fig. 4). Spreading along the Molloy ridge causes NW-SE orientation of the maximum compressive  
251 stress along most of the Vestnesa Ridge, except for the eastern segment where the influence of the Knipovich Ridge  
252 results in a rotation of the stress towards E-W (Fig. 4). It is important to wear in mind that the minimum horizontal  
253 compressive stresses ( $\sigma_h$ ) would be exerted in a plane perpendicular to the vectors in figure 4 (see Fig. 2).

254  
255 ~~The simplifying assumptions involved in our model imply that the calculated stresses in the upper crust are~~  
256 ~~unconstrained to a certain degree. However, the predicted stress directions are in general agreement with other~~  
257 ~~models of plate tectonic forces (e.g., Gölke and Coblenz, 1996; Naliboff et al., 2012), and Árnadóttir et al. (2009)~~  
258 ~~demonstrated that the deformation field from the complex plate boundary in Iceland could be modelled using~~  
259 ~~Okada's models. More importantly, a comparison of the predicted stress from plate spreading and observed~~  
260 ~~earthquake focal mechanisms shows an excellent agreement, both with regards to style and orientation of the focal~~  
261 ~~mechanisms. The earthquake focal mechanisms are mostly normal along the spreading ridges and strike-slip along~~  
262 ~~the transform faults, and the focal mechanism pressure axes align nicely with the predicted directions of maximum~~  
263 ~~compressive stress (Fig. 4). The good agreement between Okada's model and other modelling approaches as well~~  
264 ~~as between the resulting stresses and focal mechanisms in the area indicates two things: 1. that the model, despite~~  
265 ~~the simplicity of its assumptions, provides a correct first order prediction of the stress field in the upper crust, and~~  
266 ~~2. that stress from plate spreading may have a significant influence on the state of stress along the Vestnesa Ridge.~~  
267 ~~Other possible sources of stress in the region will be discussed in more detail below.~~

268 ~~The simplifying assumptions involved in the Okada models (e.g., continuous, symmetric deformation below the~~  
269 ~~brittle-ductile transition) implies that the resulting stresses are unconstrained to a certain degree. However,~~  
270 ~~Árnadóttir et al. (2009) demonstrated that the deformation field from the complex plate boundary in Iceland could~~  
271 ~~be modelled using Okada models. In addition, the predicted stress directions from Okada models are in general~~  
272 ~~agreement with other models of plate tectonic forces (e.g., Gölke & Coblenz, 1996; Naliboff et al., 2012).~~

273 Furthermore, a comparison of the predicted stress from plate spreading and observed earthquake focal mechanisms  
274 shows an excellent agreement, both with regards to style and orientation of the focal mechanisms. The earthquake  
275 focal mechanisms are mostly normal along the spreading ridges and strike slip along the transform faults, and the  
276 focal mechanism pressure axes align nicely with the predicted directions of maximum compressive stress (Fig. 4).  
277 The good agreement between Okada's and other modelling approaches as well as between the resulting stresses  
278 and focal mechanisms in the area indicates two things: 1. that the model, despite the simplicity of its assumptions,  
279 provides a correct first order prediction of the stress field in the upper crust, and 2. that stress from plate spreading  
280 may indeed have a dominant control on the stress field along the Vestnesa Ridge.

#### 282 **54.2 SPATIAL CORRELATION BETWEEN MODELLED TECTONIC STRESS REGIME, FAULTING** 283 **AND FLUID FLOW FEATURES** 284 **SEEPAGE ALONG THE VESTNSA RIDGE**

285 The zone of tensile stress on the eastern Vestnesa Ridge segment coincides with a zone of faulting and where all  
286 the present day seepage is concentrated (Fig. 3, 4). The match between the extent of the modelled tensile zone and  
287 the active pockmarks is not exact; active pockmarks exist a few kilometres westward from the termination of the  
288 tensile zone (Fig. 4). However, the agreement is striking from a regional point of view, considering the uncertainty  
289 of the model as illustrated by the sensitivity tests (Supplementary material). In the predicted tensile zone towards  
290 the east of the Vestnesa Ridge, the sub-seabed faults are NW-SE oriented, near vertical and have a gentle normal  
291 throw (< 10 m). Normal faulting or tensile opening of these faults would be enhanced by NW-SE oriented  
292 maximum compressive stress, i.e., the orientation of stresses predicted by our model on the crest and at the southern  
293 flank of the ridge until the transition to the tensile stress regime (Fig. 4). This ~~implies suggests~~ that these faults are  
294 ~~currently possibly~~ under a regime that makes them favourably permeable for fluids (Fig. 2). Indeed, these faults  
295 are spatially linked to gas chimneys and active seepage (Bünz et al., 2012; Plaza-Faverola et al., 2015). Some of  
296 the faults show thicker sediment thicknesses at the hanging wall, allowing identification of discrete periods of  
297 normal faulting (Plaza-Faverola et al., 2015).

298  
299 The character of the faults changes towards the western Vestnesa Ridge where the model predicts a strike-slip  
300 regime (Fig. 2). The density of faulting and seismic definition decreases westward (Fig. 2, 3, 5). In this part of the  
301 ridge gas chimneys are narrower, stacked more vertically than active chimneys towards the east and it is possible  
302 to recognise more faults reaching the present-day seafloor (Plaza-Faverola et al., 2015). Here, the orientation of  $\sigma_H$   
303 (NW-SE) is oblique to the more WNW-ESE to W-E oriented fault segments (Fig. 2, 4), suggesting that, with some

304 exceptions, these structures are less favourably oriented for tensile opening than the structures imaged towards the  
305 east (Fig. 2).

306

307 The cluster of larger scale N-S to NNW-SSE trending extensional faults that outcrop at the southern slope of the  
308 Vestnesa Ridge (Fig. 1, 2), also coincides with the zone of predicted tensile stress (Fig. 4). In agreement with our  
309 models, these extensional faults have been suggested to indicate the northward propagation of the Knipovich Ridge  
310 rift system (Crane et al., 2001; Vanneste et al., 2005). ~~However, it is likely that faulting along this steep slope of  
311 the Vestnesa Ridge (Fig. 1) was partially induced as well by gravitational stress.~~

312

~~313 The striking correlation between predicted tectonic stress regime, faulting structures and current seepage suggests  
314 that tectonic stress resulting from oblique spreading in the region, has potentially a major influence on the near-  
315 surface sedimentary deformation and fluid dynamics. Hereafter, we discuss the implications of the interaction  
316 between tectonic stresses and pore fluid pressure for the evolution of gas seepage along the Vestnesa Ridge.~~

317

318

319

## 320 **5.3 MODELLED STRESSES IN RELATION TO THE TOTAL STATE OF STRESS ALONG THE** 321 **VESTNESA RIDGE**

322

323

324 ~~Other sources of stress important in the region are gravitational stresses due to bathymetry/topography or  
325 subsurface density contrasts and flexural stresses due to cooling of the lithosphere or sedimentation. During the  
326 Quaternary, the west-Svalbard margin has furthermore been affected by glacially induced flexural stresses due to  
327 the glaciations (e.g., Fjeldskaar and Amantov, 2018; Patton et al., 2016).~~

328

329 ~~The topography effect on the regional stress regime appears likely along the south-eastern flank of the Vestnesa  
330 basin where the bathymetry deepens from 1200-1600 m along the crest of the Vestnesa Ridge to Ca. 2000 m near  
331 the Molloy Transform Fault (Fig. 1). Small-scale slumps at the slope (Fig 1, 2) may be evidence of gravitational  
332 forcing. Gravitational stress would induce tensile horizontal stress perpendicular to the crest of the Vestnesa ridge.  
333 Thus, faulting and opening would be induced on NW-SE trending faults on the eastern Vestnesa Ridge and WNW-  
334 ESE trending faults on the western Vestnesa Ridge. While gravitational stress may influence present day seepage~~

Formatted: Font: (Default) +Headings (Times New Roman),  
11 pt

Formatted: Font: (Default) +Headings (Times New Roman),  
11 pt, Bold, All caps

335 along the Vestnesa Ridge, it offers no explanation as to why active seepage occurs exclusively on the eastern  
336 Vestnesa Ridge.

337

338 The effect of lithospheric bending on the total state of stress in the region remains poorly investigated. It is believed  
339 that the Vestnesa sedimentary Ridge sits over relatively young oceanic crust, < 19 Ma old (Eiken and Hinz, 1993;  
340 Hustoft, 2009). The oceanic-continental transition is not well constrained but its inferred location crosses the  
341 Vestnesa Ridge at its easternmost end (Engen et al., 2008; Hustoft, 2009; Plaza-Faverola et al., 2015). This is a  
342 zone prone to flexural subsidence due to cooling during the evolution of the margin and the oceanic crust may have  
343 experienced syn-sedimentary subsidence nearby the oceanic-continental transition, as suggested for Atlantic  
344 passive margins (Turcotte et al., 1977). However, only N-S oriented faults would be consistent with a deformation  
345 incited by density contrast related flexural bending (i.e., regional structural horses and grabens are N-S trending,  
346 reflecting the direction of major rift systems during basin evolution (Faleide et al., 1991; Faleide et al., 1996).The  
347 NW-SE to E-W oriented faults on the Vestnesa Ridge point towards a different origin.

348

349 Lithospheric bending is also associated with Quaternary isostasy during glacial and interglacial periods. Glacial  
350 isostasy results in significant stresses associated with subsidence and uplift of the crust as the ice-sheet advanced  
351 or retreated. Present uplift rates are stronger at the core of the ice-sheets where the ice thickness was at the maximum  
352 (e.g., ~700 m accumulated subsidence has been estimated for the last million year at formerly glaciated basins in  
353 the Barents Sea; (Fjeldskaar and Amantov, 2018). Subsidence and uplift rates decrease towards the former ice-  
354 sheet margin. Indeed, modelled present day uplift rates at the periphery of the Barents sea ice-sheet ranges from 0  
355 to -1 mm/a, depending on the ice-sheet model used in the calculation (Auriac et al., 2016) compared to an uplift  
356 rate of up to 9 mm/a at the centre (i.e., maximum thickness zone) of the ice sheet (Auriac et al., 2016; Patton et al.,  
357 2016). Consistently, modelled glacial stresses induced by the Fennoscandian ice sheet on the mid-Norwegian  
358 margin are close to zero at present day (Lund et al., 2009; Steffen et al., 2006). The Vestnesa Ridge is located ~60  
359 km from the shelf break (Fig. 1). It is actually closer to the Molloy mid-ocean ridge than to the shelf break. It is  
360 likely that the present day effect of glacial stresses on seepage activity in the region is more important towards the  
361 seep sites on the shelf break (i.e., PKF region; Fig. 1) than along the Vestnesa Ridge. Wallmann et al., (2018)  
362 postulated that post glacial uplift lead to gas hydrate dissociation and associated seepage on the shelf break. Since  
363 no gas hydrates have been found despite deep drilling (Riedel et al., 2018), the influence of glacial stresses provides  
364 an alternative and previously not contemplated explanation for seepage in this area. It is also likely that glacial

365 stresses as far off as the Vestnesa Ridge had a more significant effect in the past, as further discussed in section  
366 4.5.

367  
368 Since we focused exclusively on modelling the type of stresses potentially generated by oblique spreading at the  
369 Molloy and Knipovich ridges, and we have so far disregarded any other source of stress, the modelled stress field  
370 in this study cannot be understood as a representation of the total state of stress in the region. However, the striking  
371 correlation between the predicted tensile stress regime with favourably oriented faults, gas chimneys and current  
372 seepage on the eastern segment of the Vestnesa Ridge, suggests that tectonic stresses resulting from oblique  
373 spreading at the Molloy and the Knipovich ridges have the potential to influence near-surface sedimentary  
374 deformation and fluid dynamics in the study area. Tectonic processes at plate margins have a major influence on  
375 regional stress patterns (Heidbach et al., 2010). Given the proximity to the Molloy and Knipovich Ridges, and  
376 without neglecting that other sources of stress can have as well a significant effect on shallow fluid dynamics, we  
377 argue that tectonic stress (ridge push) is an important factor, perhaps even a dominant factor, modulating seepage  
378 activity along the Vestnesa Ridge.

379 ~~Other stress sources of importance in the region may be gravitational stresses due to bathymetry/topography and~~  
380 ~~subsurface density contrasts and flexural stresses. During the Quaternary, the west Svalbard margin has~~  
381 ~~furthermore been affected by glacially induced flexural stresses due to the glaciations (e.g., Fjeldskaar and~~  
382 ~~Amantov, 2017; Patton et al., 2016).~~ (Auriac et al., 2016; Eiken and Hinz, 1993; Engen et al., 2008; Faleide et al.,  
383 1991; Faleide et al., 1996; Fjeldskaar and Amantov, 2018; Hustoft, 2009; Patton et al., 2016; Pedersen et al., 2010;  
384 Plaza-Faverola et al., 2015) ~~Models of stresses induced by the Fennoscandian ice sheet (Lund et al., 2009; Steffen~~  
385 ~~et al., 2006) close to zero at present day.~~

#### 387 **5.4 PRESENT DAY SEEPAGE COUPLED TO STRESS CYCLING**

388  
389 Based on the correlation between tectonic stress regimes and seepage patterns, we postulate that current seepage at  
390 the eastern Vestnesa Ridge segment is favoured by the opening of pre-existing faults in a tensile stress regime (Fig.  
391 2, 3b). Depending on the tectonic regime, permeability through faults and fractures may be enhanced or inhibited  
392 (e.g., Faulkner et al., 2010; Hillis, 2001; Sibson, 1994). Thus, spatial and temporal variations in the tectonic stress  
393 regime may control the transient release of gas from the seafloor over geological time as documented, for example,  
394 for CO<sub>2</sub> analogues in the Colorado Plateau (e.g., Jung et al., 2014).

Formatted: Normal

Formatted: Font: (Default) +Headings (Times New Roman),  
11 pt

Formatted: Font: Bold

396 It is likely that the steep NW-SE oriented faults mapped along the eastern Vestnesa Ridge segment formed in a  
397 strike-slip regime and became permeable to fluids over time. We envision that seepage is induced 1) by opening of  
398 faults favourably oriented with respect to the stress field and 2) by high pore fluid pressure at the base of the GHSZ  
399 (i.e., the shallowest reservoir holding gas from escaping to the seafloor). Thus, seepage along the Vestnesa Ridge  
400 may have been driven by cyclic changes in stress or pore fluid pressure. Opening of fractures is facilitated if the  
401 minimum horizontal stress is smaller than the pore-fluid pressure ( $p_f$ ), that is, the minimum effective stress is  
402 negative ( $\sigma_h' = \sigma_h - p_f < 0$ ) (e.g., Grauls and Baleix, 1994). Secondary permeability may increase by formation of  
403 tension fractures near damaged fault zones (Faulkner et al., 2010). A negative minimum effective stress and  
404 subsequent increase in secondary permeability in a tensile stress regime can be achieved particularly easy in the  
405 near-surface. Continued flow through opened faults and fractures would explain brecciation and development of  
406 the observed chimneys (Fig. 2b) (e.g., Sibson, 1994).

407

408 Seepage through gas chimneys has been dominantly advective and episodic (Fig. 2; Plaza-Faverola et al., 2005)  
409 likely due to consecutive decreases and increases in the pore fluid pressure at the base of the GHSZ in response to  
410 both, regional stress field variations and also to local pressure alterations associated for example with  
411 hydrofracturing (e.g., Hustoft et al., 2010 and references therein; Karstens and Berndt, 2015). Pressure increases at  
412 the base of the GHSZ in this part of the ridge is explained by a constant input of thermogenic gas from an Eocene  
413 reservoir since at least ca. 2 Ma ago (Knies et al., 2018).

414

415 The fact that there is not active seepage at present along the western Vestnesa Ridge segment (i.e., being under a  
416 strike-slip regime according to the models) is interesting, and somehow supports the notion that the tensile regime  
417 affects the fluid flow system towards the eastern segment. The lack of seepage at present in the western segment  
418 suggests that  $p_f$  at the base of the GHSZ is not high enough to overcome the minimum horizontal stress (i.e.,  $\sigma_h'$   
419 is positive) (Fig. 3a).

420

421

422

423 **5.5 PAST AND FUTURE SEEPAGE –ADDITIONAL INFLUENCE FROM GLACIAL STRESS AND**  
424 **PLATE SPREADING?**

425 **4.4 PAST SEEPAGE –AN EFFECT OF GLACIAL STRESSES?**

426

427 What triggered then seepage on the western Vestnesa Ridge and what caused the system to shut down? While  
428 tectonic stresses are constant over short geological time spans, chimney development and seafloor seepage has  
429 been a transient process because of slight variations in pore-fluid pressure (as discussed above) or the influence of  
430 other stress generating mechanisms that have repeatedly brought the system out of equilibrium. Geophysical and  
431 paleontological data indicate that there was once seepage and active chimney development on the western Vestnesa  
432 Ridge segment (e.g., Consolaro et al., 2015; Plaza-Faverola et al., 2015; Schneider et al., 2018).

433

434 Following the same explanation as for the present day seepage, the negative  $\sigma_h'$  condition could have been attained  
435 anywhere along the Vestnesa Ridge in the past due to pore fluid pressure increases at the base of the GHSZ or due  
436 to favourable stress conditions. During glacial periods, the bending forcing due to ice-loading on the lithosphere  
437 was much more significant than at present day (Lund and Schmidt, 2011). According to recent models of glacial  
438 isostasy by the Barents Sea Ice sheet during the last glacial maximum, the Vestnesa Ridge laid in a zone where  
439 subsidence could have been of tens of meters (Patton et al., 2016). At other times, before and after glacial  
440 maximums, the Vestnesa Ridge was most likely located within the isostatic forebulge.

441 ~~Following the same logic as for the present day seepage explanation, the negative  $\sigma_h'$  condition could have been~~  
442 ~~attained anywhere along the Vestnesa Ridge in the past due to pore fluid pressure increases at the base of the GHSZ~~  
443 ~~or due to a favourable orientation of the stress regime at the time. During glacial periods, the load of the ice forces~~  
444 ~~the lithosphere down and creates a forebulge along the periphery of the ice, resulting in flexural stresses in the~~  
445 ~~upper part of the lithosphere (Lund and Schmidt, 2011). The lateral expansion of grounded ice in the western~~  
446 ~~Barents Sea region is limited by the continental shelf break (Fig. 1), thus the Vestnesa Ridge may have been located~~  
447 ~~within the isostatic forebulge at given periods of times during the glaciations (Patton et al., 2016).~~

448

449 ~~We cannot conclusively argue about the potential effect of tensile stresses from current glacial isostasy over the~~  
450 ~~Vestnesa Ridge at present. However, by simple analogy with the kind of compressive stresses (magnitude and~~  
451 ~~orientation) reported beyond the shelf break off the mid-Norwegian margin for time spans close to present day ice~~  
452 ~~condition, we can sense that such an effect is minimal at present (Lund and Schmidt, 2011; Lund et al., 2009). In~~  
453 ~~general, it is expected that maximum glacially induced horizontal stresses ( $\sigma_H$ ) would be dominantly oriented~~  
454 ~~parallel to the shelf break (Björn Lund personal communication; Lund et al., 2009). This is, dominantly N-S in the~~  
455 ~~area of the Vestnesa Ridge (Fig. 1). Such stress orientation would not favour opening for fluids along pre-existing~~  
456 ~~NW-SE oriented faults associated with seepage activity at present (i.e., N-S oriented faults would be the more~~  
457 ~~vulnerable for opening). It is likely, though, that the repeated waxing and waning of the ice sheet caused a cyclic~~

458 modulation of the stress field (varying magnitude and orientation) and influenced the dynamics of gas  
459 accumulations and favourably oriented faults along the Vestnesa Ridge in the past. Past glacial stresses may provide  
460 ~~them~~ an alternative explanation for seepage along the entire Vestnesa Ridge extent at given periods of time (Fig.  
461 5); in line with the correlation between seepage and glacial-interglacial events postulated for different continental  
462 margins e.g., for chimneys off the mid-Norwegian margin (Plaza-Faverola et al., 2011), the Gulf of Lion (Riboulot  
463 et al., 2014), but also along the Vestnesa Ridge (Plaza-Faverola et al., 2015; Schneider et al., 2018).

464

465

466 The temporal variation in the stress field along the Vestnesa Ridge is also caused by its location on a constantly  
467 growing plate. As the oceanic plate grows, the Vestnesa Ridge moves eastward with respect to the Molloy and  
468 Knipovich Ridges, causing a westward shift in the regional stress field on the Vestnesa Ridge (Fig. 6). In the future,  
469 the eastern Vestnesa Ridge may temporarily move out of the tensile zone, while the western Vestnesa Ridge moves  
470 into it (Fig. 6). This suggests that a negative effective stress and subsequent active seepage may reappear at  
471 pockmarks to the west of the currently active seepage zone.

472

473 ~~The effect of glacial stresses over the fluid flow system off west Svalbard will be further tested (at least for the~~  
474 ~~Weichselian period) by implementing Lund et al., models using newly constrained Barents Sea ice sheet models~~  
475 ~~(Patton et al., 2016). Additional sources of stress related to topography/bathymetry should be further investigated~~  
476 ~~as well to gain a comprehensive assessment of the effect of the total stress field on near surface fluid migration in~~  
477 ~~the region.~~

478

## 479 **6- CONCLUSIONS**

480

481 ~~Analytical modelling of the stress field generated by oblique spreading at the Molloy and Knipovich ridges in the~~  
482 ~~Fram Strait, suggests that tectonic forcing may be an important factor controlling faulting and seepage distribution~~  
483 ~~along the Vestnesa Ridge, off the west-Svalbard margin. Other important sources of stress such as bathymetry and~~  
484 ~~lithospheric bending, contributing to the actual state of stress off Svalbard, are not considered in the modelling~~  
485 ~~exercise presented here; thus, we cannot quantitatively assess whether ridge push has a dominant effect on seepage~~  
486 ~~activity. However, our analysis of how stress from plate spreading may affect mapped faults along the Vestnesa~~  
487 ~~Ridge suggests that a spatial variation in the tectonic stress regime favours fluid migration through faults on the~~  
488 ~~eastern Vestnesa Ridge where active seepage occurs. We suggest that present-day seepage is facilitated by opening~~

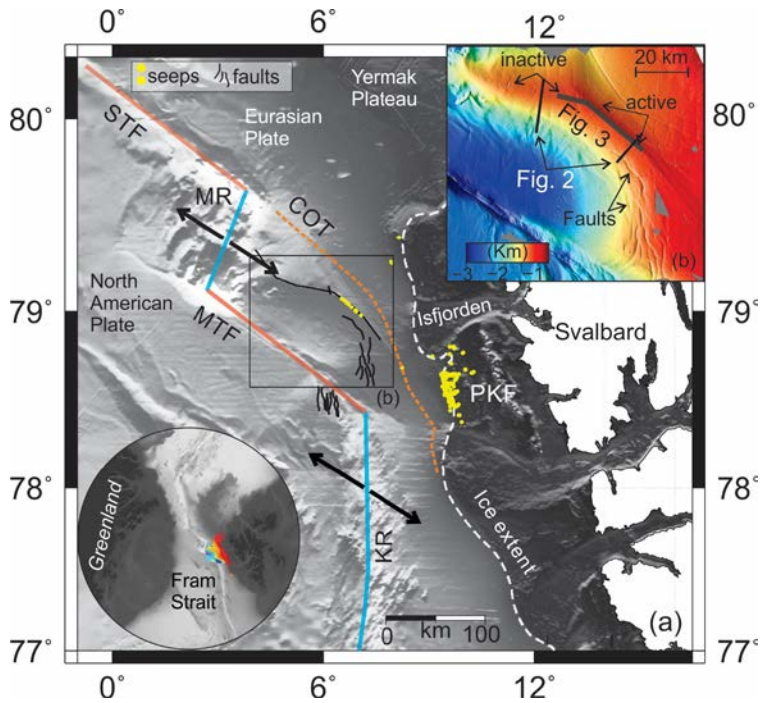
489 of faults and fractures in a tensile stress regime or dilation on faults favourably oriented with respect to principal  
490 stresses, where pore fluid pressure overcomes the minimum horizontal stress. Multiple seepage events along the  
491 entire extent of the Vestnesa Ridge, may have been induced by additional sources of stress likely associated with  
492 glacial isostasy. Future reactivation of currently dormant pockmarks is likely following the gradual westward  
493 propagation of the tensile stress zone on the Vestnesa Ridge as the Eurasian plate drift towards the south-east.  
494 Despite the simplifying assumptions by the analytical model approach implemented here, this study provides a first  
495 order assessment of how important understanding the state of stress is for reconstructing seepage activity in Arctic  
496 passive margins.

497 ~~The results of modelling the stress regime generated exclusively by mid-ocean ridge spreading in the Fram Strait~~  
498 ~~support seismic evidence of the correlation between faulting and seepage distribution along the Vestnesa~~  
499 ~~sedimentary ridge, offshore the west-Svalbard margin. Tectonic stresses due to oblique spreading along the Molloy~~  
500 ~~and the Knipovich ridges influences the present day stress field across the west-Svalbard passive margin. A~~  
501 ~~correlation between a tensile stress regimes and seepage activity suggests that episodic seepage through gas~~  
502 ~~chimneys has been controlled by an interplay between varying minimum horizontal stresses and pore fluid pressure~~  
503 ~~at the free gas zone beneath the gas hydrate reservoir. Our study suggests that present day seepage is facilitated by~~  
504 ~~opening of faults and fractures in a tensile stress regime or dilation on faults favourably oriented in a strike slip~~  
505 ~~regime, where pore fluid pressure overcomes the minimum horizontal stress. Multiple seepage events along the~~  
506 ~~entire extent of the Vestnesa Ridge, may have been triggered either by favourable orientation of faults with respect~~  
507 ~~to mid-ocean ridge derived stresses in the past or by additional sources of stress related for example to glacial~~  
508 ~~isostasy. Future reactivation of currently dormant pockmarks is likely following the gradual westward propagation~~  
509 ~~of the tensile stress zone on the Vestnesa Ridge as the Eurasian plate drift towards the south-east.~~

## 511 **7- OUTLOOK**

512 The effect of glacial stresses over the fluid flow system off west-Svalbard will be further tested (at least for the  
513 Weichselian period) by implementing Lund et al., models using newly constrained Barents Sea ice-sheet models  
514 (Patton et al., 2016). Additional sources of stress related to topography/bathymetry should be further investigated  
515 as well to gain a comprehensive assessment of the effect of the total stress field on near-surface fluid migration in  
516 the region.

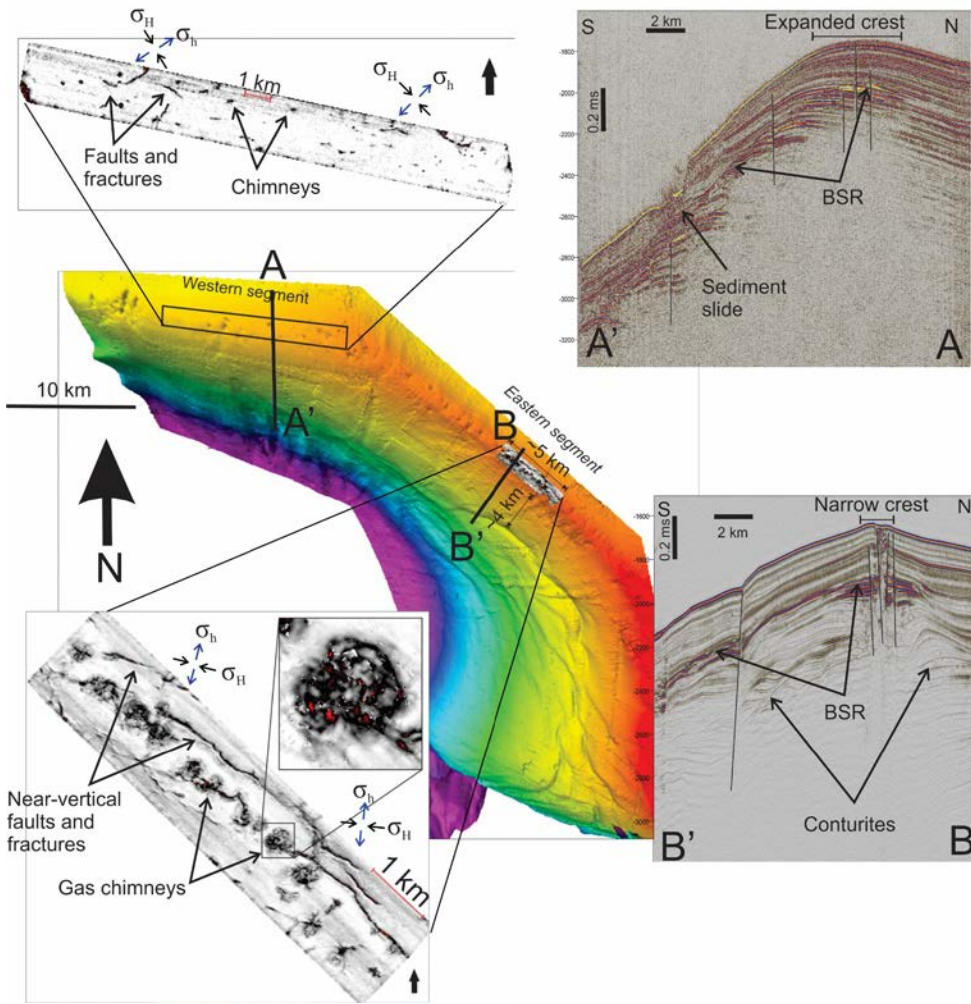
## 519 **Figures**



520  
 521 **Figure 1:** (a) International Bathymetry Chart of the Arctic Ocean (IBCAO) showing the geometry of mid-ocean  
 522 ridges offshore the west-Svalbard margin; (b) High resolution bathymetry along the Vestnesa Ridge (UiT, R/V HH  
 523 multi-beam system). Seafloor pockmarks are observed along the entire ridge but active seep sites are restricted to  
 524 its eastern segment; PKF=Prins Karl Foreland; STF=Spitsbergen Transform Fault; MR=Molloy Ridge;  
 525 MTF=Molloy Transform Fault; KR=Knipovich Ridge; COT=Continental-Oceanic Transition (Engen et al., 2008);  
 526 Ice-Sheet Extent (Patton et al., 2016).

527  
 528  
 529  
 530  
 531  
 532

533



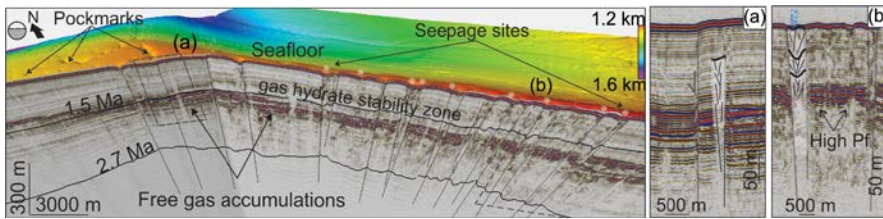
534

535

Formatted: English (United States)

536 Figure 2: Composite figure with bathymetry and variance maps from 3D seismic data along the eastern and the  
 537 western Vestnesa Ridge segments (modified from Plaza-Faverola et al., 2015). The orientation of maximum  
 538 compressive horizontal stress ( $\sigma_H$ ) and minimum horizontal stress ( $\sigma_h$ ) predicted by the model are projected ~~over~~  
 539 ~~selected~~ ~~for comparison with fault segments orientations~~. Notice the favourable orientation of stresses for opening  
 540 to fluids along faults on the eastern Vestnesa Ridge segment. Two-2D seismic transects (A-A' - Büinz et al., 2012  
 541 and B-B' - Johnson et al., 2015) illustrate the morphological difference of the crest of the Vestnesa Ridge (i.e.,  
 542 narrow vs. extended) believed to be determined by bottom current dominated deposition and erosion (Eiken and  
 543 Hinz, 1993).

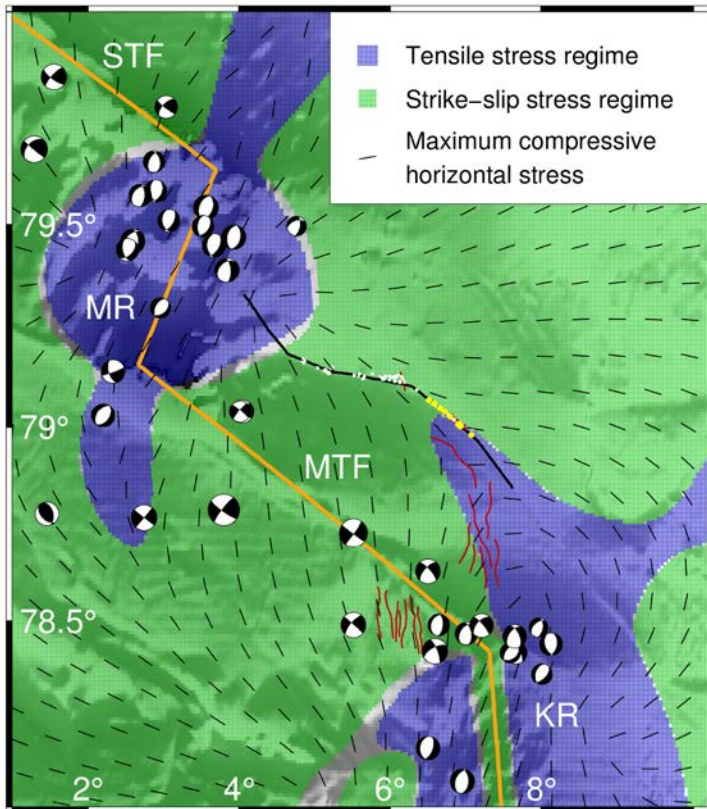
544



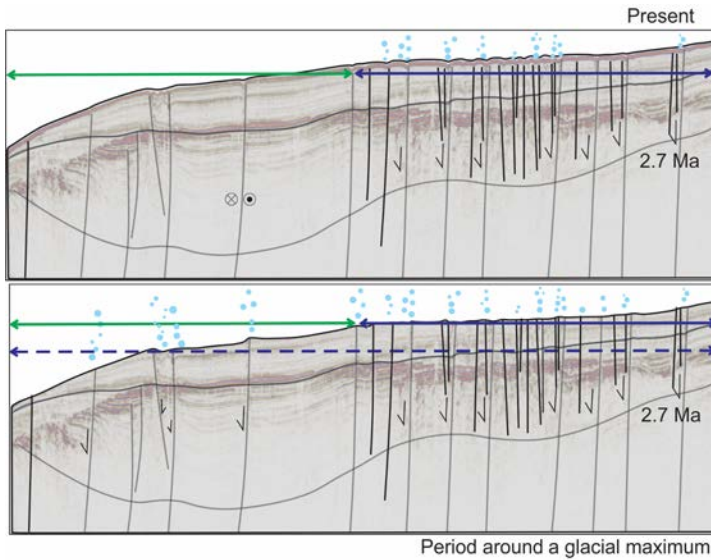
545

546 **Figure 3:** Integrated seismic and bathymetry image of the gas hydrate system along the Vestnesa Ridge. (a)  
 547 Outcropping fault located at the transition from the active to the currently inactive pockmark region; (b) Gas  
 548 chimneys with active seepage and inferred high pore-fluid pressure (Pf) zone.

549



550  
 551 **Figure 4:** Modelled upper crustal tectonic stress field (blue – tensile and green - strike-slip regime) and stress  
 552 orientations, due to oblique spreading at Molloy Ridge (MR) and Knipovich Ridge (KR). The seismic line is  
 553 projected as reference for the crest of the Vestnesa Ridge. Red lines are faults, yellow dots seeps and white circles  
 554 inactive pockmarks. The focal mechanisms are from the ISC Online Bulletin (<http://www.isc.ac.uk>).



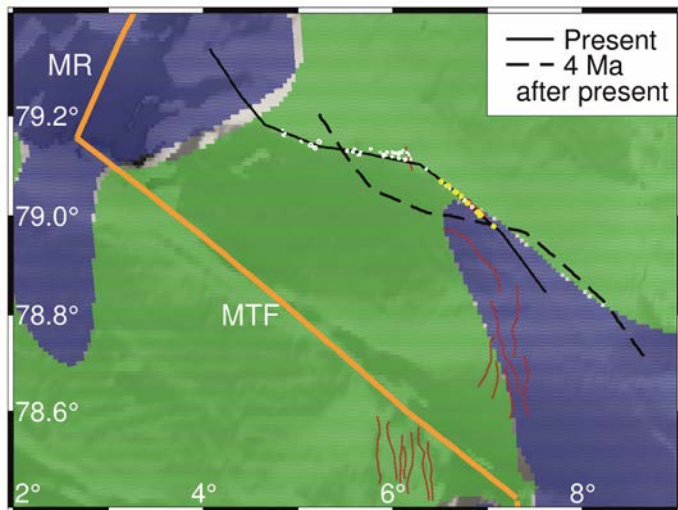
555

556 **Figure 5:** Conceptual model of the evolution of seepage coupled to faulting and spatial variations in the stress  
 557 regime (tensile=blue; strike-slip=green) along the Vestnesa Ridge, offshore the west-Svalbard margin. At present  
 558 day, tensile stress from mid-ocean ridge spreading (blue solid line) favours seepage exclusively on the eastern  
 559 segment of the Vestnesa Ridge. Seepage on the western Vestnesa Ridge and other regions may have been induced  
 560 repeatedly since the onset of glaciations 2.7 Ma ago (Mattingsdal et al., 2014), due to tensional flexural stresses  
 561 in the isostatic forebulge around the time of glacial maximums.

562

563

564



565

566 **Figure 6:** Stress field in figure 3 showing the location of the Vestnesa Ridge at present and 4 Ma after present time,  
 567 assuming a constant spreading velocity of 7 mm/yr in the direction N125°E. The black polygon corresponds to the  
 568 seismic line in Plaza-Faverola et al., 2017 and partly shown in figure 3. It is presented as reference for the crest of  
 569 the eastern and western Vestnesa Ridge segments

570

## 571 **Appendix A**

### 572 **Model description**

573

574 We use the analytical formulations of Okada (1985) for a finite rectangular dislocation source in elastic  
 575 homogeneous isotropic half-space (Fig. A.1). The dislocation source can be used to approximate deformation along  
 576 planar surfaces, such as volcanic dykes (e.g. Wright et al., 2006), sills (e.g. Pedersen and Sigmundsson, 2004),  
 577 faults (e.g. Massonet et al, 1993) and spreading ridges (e.g. Keiding et al., 2009). More than one dislocations can  
 578 be combined to obtain more complex geometry of the source or varying deformation along a planar source. The  
 579 deformation of the source can be defined as either lateral shear (strike-slip for faults), vertical shear (dip-slip at  
 580 faults) or tensile opening.

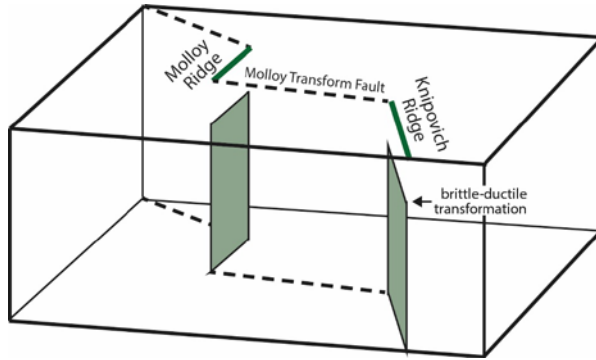
581

582 The Okada model assumes flat Earth without inhomogeneities. While the flat-earth assumption is usually adequate  
 583 for regional studies (e.g. Wolf, 1984), the lateral inhomogeneities can sometimes cause considerable effect on the  
 584 deformation field (e.g. Okada, 1985). However, the dislocation model is useful as a first approximation to the  
 585 problem.

586

587 At mid-ocean ridges, deformation is driven by the continuous spreading caused primarily by gravitational stress  
 588 due to the elevation of the ridges, but also basal drag and possibly slab pull. Deformation occurs continuously in  
 589 the ductile part of the crust. Meanwhile, elastic strain builds in the upper, brittle part of the crust. To model this  
 590 setting, the upper boundary of the dislocation source must be located at the depth of the brittle-ductile transition  
 591 zone. The lower boundary of the source is set to some arbitrary large depth to avoid boundary effects.

592



593

594 **Fig A.1 Extract of model showing the location of the dislocation sources (light green) for Molloy and**  
 595 **Knipovich ridges. Note that the model is an infinite half-space, i.e. it has no lateral or lower boundary.**

596

597 The Okada model provides the displacements  $u_x, u_y, u_z$  (or velocities if deformation is time-dependent) at defined  
 598 grid points at the surface and subsurface. It also provides strain (or strain rates) defined as:

599

$$\varepsilon_{ij} = \frac{1}{2}(u_{i,j} + u_{j,i})$$

600 The stress field can then be calculated from the predicted strain rates. In homogeneous isotropic media, stress is  
 601 related to strain as:

602

$$\sigma_{ij} = \lambda \delta_{ij} \varepsilon_{kk} + 2\mu \varepsilon_{ij}$$

603 where  $\delta_{ij}$  if the Kronecker delta,  $\lambda$  is Lamé's first parameter, and  $\mu$  is the shear modulus. Lamé's first parameter  
604 does not have a physical meaning but is related to the shear modulus and Poisson's ratio ( $\nu$ ) as  $\lambda = \frac{2\mu\nu}{1-2\nu}$ .  
605 The absolute values of stress are in general difficult to model (e.g. Hergert and Heidbach, 2011), and not possible  
606 with our analytical model. However, the model provides us with the orientations and relative magnitude of the  
607 stresses. That is, we know the relative magnitudes of the vertical stress ( $\sigma_v$ ), maximum horizontal stress ( $\sigma_H$ ) and  
608 minimum horizontal stress ( $\sigma_h$ ). From this, the stress regime can be defined as either tensile ( $\sigma_v > \sigma_H > \sigma_h$ ), strike-  
609 slip ( $\sigma_H > \sigma_v > \sigma_h$ ) or compressive ( $\sigma_H > \sigma_h > \sigma_v$ ).

610

#### 611 **Author contribution**

612 Andreia Plaza-Faverola conceived the paper idea. She is responsible for seismic data processing and interpretation.

613 Marie Keiding did the tectonic modelling. The paper is the result of integrated work between both.

614

#### 615 **ACKNOWLEDGEMENTS**

616 This research is part of the Centre for Arctic Gas Hydrate, Environment and Climate (CAGE) supported by the  
617 Research Council of Norway through its Centres of Excellence funding scheme grant No. 223259. Marie Keiding  
618 is supported by the NEONOR2 project at the Geological Survey of Norway. Special thanks to Björn Lund, Peter  
619 Schmidt, Henry Patton, and Alun Hubbard for their interest in the present project and constructive discussions  
620 about isostasy and glacial stresses. We are thankful to various reviewers that have contributed to the improvement  
621 of the manuscript. Seismic data is archived at CAGE – Centre for Arctic Gas Hydrate, Environment and Climate,  
622 Tromsø, Norway and can be made available by contacting APF. Modelled stresses can be made available by  
623 contacting MK.

624

#### 625 **References:**

626 Ambrose, W.G., Panieri, G., Schneider, A., Plaza-Faverola, A., Carroll, M.L., Åström, E.K., Locke, W.L., Carroll, J.,  
627 2015. Bivalve shell horizons in seafloor pockmarks of the last glacial-interglacial transition: a thousand years of  
628 methane emissions in the Arctic Ocean. *Geochemistry, Geophysics, Geosystems* 16, 4108-4129.  
629 Andreassen, K., Hubbard, A., Winsborrow, M., Patton, H., Vadakkepuliambatta, S., Plaza-Faverola, A.,  
630 Gudlaugsson, E., Serov, P., Deryabin, A., Mattingdal, R., 2017. Massive blow-out craters formed by hydrate-  
631 controlled methane expulsion from the Arctic seafloor. *Science* 356, 948-953.  
632 Árnadóttir, T., Lund, B., Jiang, W., Geirsson, H., Björnsson, H., Einarsson, P., Sigurdsson, T., 2009. Glacial  
633 rebound and plate spreading: results from the first countrywide GPS observations in Iceland. *Geophysical*  
634 *Journal International* 177, 691-716.

635 Auriac, A., Whitehouse, P., Bentley, M., Patton, H., Lloyd, J., Hubbard, A., 2016. Glacial isostatic adjustment  
636 associated with the Barents Sea ice sheet: a modelling inter-comparison. *Quaternary Science Reviews* 147, 122-  
637 135.

638 Bünz, S., Polyanov, S., Vadakkepuliambatta, S., Consolaro, C., Mienert, J., 2012. Active gas venting through  
639 hydrate-bearing sediments on the Vestnesa Ridge, offshore W-Svalbard. *Marine geology*.

640 Consolaro, C., Rasmussen, T., Panieri, G., Mienert, J., Bünz, S., Szybor, K., 2015. Carbon isotope ( $\delta^{13}C$ )  
641 excursions suggest times of major methane release during the last 14 kyr in Fram Strait, the deep-water  
642 gateway to the Arctic. *Climate of the Past* 11, 669-685.

643 Crane, K., Doss, H., Vogt, P., Sundvor, E., Cherkashov, G., Poroshina, I., Joseph, D., 2001. The role of the  
644 Spitsbergen shear zone in determining morphology, segmentation and evolution of the Knipovich Ridge. *Marine*  
645 *geophysical researches* 22, 153-205.

646 Crane, K., Sundvor, E., Buck, R., Martinez, F., 1991. Rifting in the northern Norwegian-Greenland Sea: Thermal  
647 tests of asymmetric spreading. *Journal of Geophysical Research: Solid Earth* 96, 14529-14550.

648 DeMets, C., Gordon, R.G., Argus, D.F., 2010. Geologically current plate motions. *Geophysical Journal*  
649 *International* 181, 1-80.

650 Dickens, G.R., 2011. Down the rabbit hole: Toward appropriate discussion of methane release from gas hydrate  
651 systems during the Paleocene-Eocene thermal maximum and other past hyperthermal events. *Climate of the*  
652 *Past* 7, 831-846.

653 Ehlers, B.-M., Jokat, W., 2009. Subsidence and crustal roughness of ultra-slow spreading ridges in the northern  
654 North Atlantic and the Arctic Ocean. *Geophysical Journal International* 177, 451-462.

655 Eiken, O., Hinz, K., 1993. Contourites in the Fram Strait. *Sedimentary Geology* 82, 15-32.

656 Eldholm, O., Faleide, J.I., Myhre, A.M., 1987. Continent-ocean transition at the western Barents Sea/Svalbard  
657 continental margin. *Geology* 15, 1118-1122.

658 Engen, Ø., Faleide, J.I., Dyreng, T.K., 2008. Opening of the Fram Strait gateway: A review of plate tectonic  
659 constraints. *Tectonophysics* 450, 51-69.

660 Faleide, J., Gudlaugsson, S., Eldholm, O., Myhre, A., Jackson, H., 1991. Deep seismic transects across the sheared  
661 western Barents Sea-Svalbard continental margin. *Tectonophysics* 189, 73-89.

662 Faleide, J.I., Solheim, A., Fiedler, A., Hjelstuen, B.O., Andersen, E.S., Vanneste, K., 1996. Late Cenozoic evolution  
663 of the western Barents Sea-Svalbard continental margin. *Global and Planetary Change* 12, 53-74.

664 Faulkner, D., Jackson, C., Lunn, R., Schlische, R., Shipton, Z., Wibberley, C., Withjack, M., 2010. A review of  
665 recent developments concerning the structure, mechanics and fluid flow properties of fault zones. *Journal of*  
666 *Structural Geology* 32, 1557-1575.

667 Fjeldskaar, W., Amantov, A., 2017. Effects of glaciations on sedimentary basins. *Journal of Geodynamics*.

668 Fjeldskaar, W., Amantov, A., 2018. Effects of glaciations on sedimentary basins. *Journal of Geodynamics* 118,  
669 66-81.

670 Gaina, C., Nikishin, A., Petrov, E., 2015. Ultraslow spreading, ridge relocation and compressional events in the  
671 East Arctic region: A link to the Eureka orogeny? *arctos* 1, 16.

672 Geersen, J., Scholz, F., Linke, P., Schmidt, M., Lange, D., Behrmann, J.H., Völker, D., Hensen, C., 2016. Fault zone  
673 controlled seafloor methane seepage in the rupture area of the 2010 Maule Earthquake, Central Chile.  
674 *Geochemistry, Geophysics, Geosystems* 17, 4802-4813.

675 Grauls, D., Baleix, J., 1994. Role of overpressures and in situ stresses in fault-controlled hydrocarbon migration:  
676 A case study. *Marine and Petroleum Geology* 11, 734-742.

Formatted: Norwegian (Bokmål)

Formatted: Norwegian (Bokmål)

677 Grunnaleite, I., Fjeldskaar, W., Wilson, J., Faleide, J., Zweigel, J., 2009. Effect of local variations of vertical and  
678 horizontal stresses on the Cenozoic structuring of the mid-Norwegian shelf. *Tectonophysics* 470, 267-283.

679 Gölke, M., Coblenz, D., 1996. Origins of the European regional stress field. *Tectonophysics* 266, 11-24.

680 Heidbach, O., Rajabi, M., Reiter, K., Ziegler, M., 2016. World stress map 2016. *Science* 277, 1956-1962.

681 Heidbach, O., Tingay, M., Barth, A., Reinecker, J., Kurfeß, D., Müller, B., 2010. Global crustal stress pattern based  
682 on the World Stress Map database release 2008. *Tectonophysics* 482, 3-15.

683 Hillis, R.R., 2001. Coupled changes in pore pressure and stress in oil fields and sedimentary basins. *Petroleum*  
684 *Geoscience* 7, 419-425.

685 Hunter, S., Goldobin, D., Haywood, A., Ridgwell, A., Rees, J., 2013. Sensitivity of the global submarine hydrate  
686 inventory to scenarios of future climate change. *Earth and Planetary Science Letters* 367, 105-115.

687 Hustoft, S., Bunz, S., Mienert, J., Chand, S., 2009. Gas hydrate reservoir and active methane-venting province in  
688 sediments on < 20 Ma young oceanic crust in the Fram Strait, offshore NW-Svalbard. *Earth and Planetary*  
689 *Science Letters* 284, 12-24.

690 Hustoft, S., Bünz, S., Mienert, J., 2010. Three-dimensional seismic analysis of the morphology and spatial  
691 distribution of chimneys beneath the Nyegga pockmark field, offshore mid-Norway. *Basin Research* 22, 465-  
692 480.

693 Jakobsson, M., Backman, J., Rudels, B., Nycander, J., Frank, M., Mayer, L., Jokat, W., Sangiorgi, F., O'Regan, M.,  
694 Brinkhuis, H., 2007. The early Miocene onset of a ventilated circulation regime in the Arctic Ocean. *Nature* 447,  
695 986-990.

696 Jansen, E., Sjøholm, J., 1991. Reconstruction of glaciation over the past 6 Myr from ice-borne deposits in the  
697 Norwegian Sea. *Nature* 349, 600.

698 Jansen, E., Sjøholm, J., Bleil, U., Erichsen, J., 1990. Neogene and Pleistocene glaciations in the northern  
699 hemisphere and late Miocene—Pliocene global ice volume fluctuations: Evidence from the Norwegian Sea,  
700 *Geological History of the Polar Oceans: Arctic versus Antarctic*. Springer, pp. 677-705.

701 Johnson, J.E., Mienert, J., Plaza-Faverola, A., Vadakkepuliymbatta, S., Knies, J., Bünz, S., Andreassen, K., Ferré,  
702 B., 2015. Abiotic methane from ultraslow-spreading ridges can charge Arctic gas hydrates. *Geology*, G36440.  
703 36441.

704 Judd, A., Hovland, M., 2009. Seabed fluid flow: the impact on geology, biology and the marine environment.  
705 Cambridge University Press.

706 Jung, N.-H., Han, W.S., Watson, Z., Graham, J.P., Kim, K.-Y., 2014. Fault-controlled CO<sub>2</sub> leakage from natural  
707 reservoirs in the Colorado Plateau, East-Central Utah. *Earth and Planetary Science Letters* 403, 358-367.

708 Karstens, J., Berndt, C., 2015. Seismic chimneys in the Southern Viking Graben—Implications for palaeo fluid  
709 migration and overpressure evolution. *Earth and Planetary Science Letters* 412, 88-100.

710 Keiding, M., Lund, B., Árnadóttir, T., 2009. Earthquakes, stress, and strain along an obliquely divergent plate  
711 boundary: Reykjanes Peninsula, southwest Iceland. *Journal of Geophysical Research: Solid Earth* 114.

712 Knies, J., Daszinnies, M., Plaza-Faverola, A., Chand, S., Sylta, Ø., Bünz, S., Johnson, J.E., Mattingsdal, R., Mienert,  
713 J., 2018. Modelling persistent methane seepage offshore western Svalbard since early Pleistocene. *Marine and*  
714 *Petroleum Geology* 91, 800-811.

715 Knies, J., Matthiessen, J., Vogt, C., Laberg, J.S., Hjelstuen, B.O., Smelror, M., Larsen, E., Andreassen, K., Eidvin, T.,  
716 Vorren, T.O., 2009. The Plio-Pleistocene glaciation of the Barents Sea–Svalbard region: a new model based on  
717 revised chronostratigraphy. *Quaternary Science Reviews* 28, 812-829.

718 Lund, B., Schmidt, P., 2011. Stress evolution and fault stability at Olkiluoto during the Weichselian glaciation.  
719 Posiva Oy.

720 Lund, B., Schmidt, P., Hieronymus, C., 2009. Stress evolution and fault stability during the Weichselian glacial  
721 cycle. Swedish Nuclear Fuel and Waste Management Co, Stockholm, Sweden.

722 Lund, B., Townend, J., 2007. Calculating horizontal stress orientations with full or partial knowledge of the  
723 tectonic stress tensor. *Geophysical Journal International* 170, 1328-1335.

724 Mattingsdal, R., Knies, J., Andreassen, K., Fabian, K., Husum, K., Grøsfjeld, K., De Schepper, S., 2014. A new 6  
725 Myr stratigraphic framework for the Atlantic–Arctic Gateway. *Quaternary Science Reviews* 92, 170-178.

726 Morgan, W.J., 1981. 13. Hotspot tracks and the opening of the Atlantic and Indian Oceans. *The oceanic*  
727 *lithosphere* 7, 443.

728 Myhre, A.M., Eldholm, O., 1988. The western Svalbard margin (74–80 N). *Marine and Petroleum Geology* 5, 134-  
729 156.

730 Naliboff, J., Lithgow-Bertelloni, C., Ruff, L., de Koker, N., 2012. The effects of lithospheric thickness and density  
731 structure on Earth' s stress field. *Geophysical Journal International* 188, 1-17.

732 Nasuti, A., Olesen, O., 2014. Chapter 4: Magnetic data. In: Hopper J.R., Funck T., Stoker T., Arting U., Peron-  
733 Pinvidic G., Doornebal H. & Gaina C. (eds) *Tectonostratigraphic Atlas of the North-East Atlantic Region*.  
734 Geological Survey of Denmark and Greenland (GEUS), Copenhagen, Denmark, 41–51. .

735 Okada, Y., 1985. Surface deformation due to shear and tensile faults in a half-space. *Bulletin of the*  
736 *seismological society of America* 75, 1135-1154.

737 Patton, H., Hubbard, A., Andreassen, K., Winsborrow, M., Stroeven, A.P., 2016. The build-up, configuration, and  
738 dynamical sensitivity of the Eurasian ice-sheet complex to Late Weichselian climatic and oceanic forcing.  
739 *Quaternary Science Reviews* 153, 97-121.

740 Pedersen, R.B., Rapp, H.T., Thorseth, I.H., Lilley, M.D., Barriga, F.J., Baumberger, T., Flesland, K., Fonseca, R.,  
741 Früh-Green, G.L., Jorgensen, S.L., 2010. Discovery of a black smoker vent field and vent fauna at the Arctic Mid-  
742 Ocean Ridge. *Nature Communications* 1, 126.

743 Petersen, C.J., Bünz, S., Hustoft, S., Mienert, J., Klaeschen, D., 2010. High-resolution P-Cable 3D seismic imaging  
744 of gas chimney structures in gas hydrated sediments of an Arctic sediment drift. *Marine and Petroleum Geology*  
745 doi: 10.1016/j.marpetgeo.2010.06.006, 1-14.

746 Planke, S., Eriksen, F.N., Berndt, C., Mienert, J., Masson, D., 2009. P-Cable high-resolution seismic.  
747 *Oceanography* 22, 85.

748 Plaza-Faverola, A., Bünz, S., Mienert, J., 2011. Repeated fluid expulsion through sub-seabed chimneys offshore  
749 Norway in response to glacial cycles. *Earth and Planetary Science Letters* 305, 297-308.

750 Plaza-Faverola, A., Bünz, S., Johnson, J.E., Chand, S., Knies, J., Mienert, J., Franek, P., 2015. Role of tectonic  
751 stress in seepage evolution along the gas hydrate-charged Vestnesa Ridge, Fram Strait. *Geophysical Research*  
752 *Letters* 42, 733-742.

753 Plaza-Faverola, A., Henrys, S., Pecher, I., Wallace, L., Klaeschen, D., 2016. Splay fault branching from the  
754 Hikurangi subduction shear zone: Implications for slow slip and fluid flow. *Geochemistry, Geophysics,*  
755 *Geosystems* 17, 5009-5023.

756 Plaza-Faverola, A., Vadakkepuliymbatta, S., Hong, W.L., Mienert, J., Bünz, S., Chand, S., Greinert, J., 2017.  
757 Bottom-simulating reflector dynamics at Arctic thermogenic gas provinces: an example from Vestnesa Ridge,  
758 offshore west-Svalbard. *Journal of Geophysical Research: Solid Earth*.

759 Portnov, A., Vadakkepuliymbatta, S., Mienert, J., Hubbard, A., 2016. Ice-sheet-driven methane storage and  
760 release in the Arctic. *Nature communications* 7.

761 Riboulot, V., Thomas, Y., Berné, S., Jouet, G., Cattaneo, A., 2014. Control of Quaternary sea-level changes on gas  
762 seeps. *Geophysical Research Letters* 41, 4970-4977.

Formatted: French (France)

763 Riedel, M., Wallmann, K., Berndt, C., Pape, T., Freudenthal, T., Bergenthal, M., Bünz, S., Bohrmann, G., 2018. In  
764 situ temperature measurements at the Svalbard Continental Margin: Implications for gas hydrate dynamics.  
765 *Geochemistry, Geophysics, Geosystems* 19, 1165-1177.

766 Roy, S., Senger, K., Braathen, A., Noormets, R., Hovland, M., Olausson, S., 2014. Fluid migration pathways to  
767 seafloor seepage in inner Isfjorden and Adventfjorden, Svalbard. Geological controls on fluid flow and seepage  
768 in western Svalbard fjords, Norway. An integrated marine acoustic study.

769 Schiffer, C., Tegner, C., Schaeffer, A.J., Pease, V., Nielsen, S.B., 2018. High Arctic geopotential stress field and  
770 implications for geodynamic evolution. Geological Society, London, Special Publications 460, 441-465.

771 Schneider, A., Panieri, G., Lepland, A., Consolaro, C., Crémère, A., Forwick, M., Johnson, J.E., Plaza-Faverola, A.,  
772 Sauer, S., Knies, J., 2018. Methane seepage at Vestnesa Ridge (NW Svalbard) since the Last Glacial Maximum.  
773 *Quaternary Science Reviews* 193, 98-117.

774 Sibson, R.H., 1994. Crustal stress, faulting and fluid flow. Geological Society, London, Special Publications 78, 69-  
775 84.

776 Skarke, A., Ruppel, C., Kodis, M., Brothers, D., Lobecker, E., 2014. Widespread methane leakage from the sea  
777 floor on the northern US Atlantic margin. *Nature Geoscience* 7, 657-661.

778 Smith, A.J., Mienert, J., Bünz, S., Greinert, J., 2014. Thermogenic methane injection via bubble transport into the  
779 upper Arctic Ocean from the hydrate-charged Vestnesa Ridge, Svalbard. *Geochemistry, Geophysics,*  
780 *Geosystems*.

781 Steffen, H., Kaufmann, G., Wu, P., 2006. Three-dimensional finite-element modeling of the glacial isostatic  
782 adjustment in Fennoscandia. *Earth and Planetary Science Letters* 250, 358-375.

783 Svensen, H., Planke, S., Malthe-Sørensen, A., Jamtveit, B., Myklebust, R., Eidem, T.R., Rey, S.S., 2004. Release of  
784 methane from a volcanic basin as a mechanism for initial Eocene global warming. *Nature* 429, 542-545.

785 Turcotte, D., Ahern, J., Bird, J., 1977. The state of stress at continental margins. *Tectonophysics* 42, 1-28.

786 Turcotte, D.L., Schubert, G., 2002. *Geodynamics*. Cambridge University Press.

787 Vanneste, M., Guidard, S., Mienert, J., 2005. Arctic gas hydrate provinces along the western Svalbard  
788 continental margin. *Norwegian Petroleum Society Special Publications* 12, 271-284.

789 Vogt, P.R., Crane, K., Sundvor, E., Max, M.D., Pfirman, S.L., 1994. Methane-generated (?) pockmarks on young,  
790 thickly sedimented oceanic crust in the Arctic: Vestnesa ridge, Fram strait. *Geology* 22, 255-258.

791 Wallmann, K., Riedel, M., Hong, W., Patton, H., Hubbard, A., Pape, T., Hsu, C., Schmidt, C., Johnson, J., Torres,  
792 M., 2018. Gas hydrate dissociation off Svalbard induced by isostatic rebound rather than global warming.  
793 *Nature communications* 9, 83.

794 Westbrook, G.K., Thatcher, K.E., Rohling, E.J., Piotrowski, A.M., Palike, H., Osborne, A.H., Nisbet, E.G., Minshull,  
795 T.A., Lanoiselle, M., James, R.H., Huhnerbach, V., Green, D., Fisher, R.E., Crocker, A.J., Chabert, A., Bolton, C.,  
796 Beszczynska-Moller, A., Berndt, C., Aquilina, A., 2009. Escape of methane gas from the seabed along the West  
797 Spitsbergen continental margin. *Geophysical Research Letters* 36, 5.

798 Zoback, M.D., Zoback, M.L., 2002. 34 State of stress in the Earth's lithosphere. *International Geophysics* 81, 559-  
799 XII.

Formatted: Norwegian (Bokmål)

Formatted: Norwegian (Bokmål)

800